East Asian Journal on Applied Mathematics
doi: 10.4208/eajam.2022-307.090123

Vol. **13**, No. 3, pp. 550-575
August 2023

A New Class of Efficient SAV Schemes with Lagrange Multipliers for Dissipative Systems with Global Constraints

Yanrong Zhang[1,2] and Jie Shen[1,3,*]

[1]*School of Mathematical Sciences and Fujian Provincial Key Laboratory on Mathematical Modeling and High Performance Scientific Computing, Xiamen University, Xiamen, Fujian, 361005, China.*
[2]*Department of Applied Mathematics, The Hong Kong Polytechnic University, Hung Hom, Hong Kong SAR, China.*
[3]*Department of Mathematics, Purdue University, West Lafayette, IN 47907, USA.*

Received 5 November 2022; Accepted (in revised version) 9 January 2023.

Dedicated to Professor Tao Tang on occasion of his 60th birthday.

Abstract. In this paper, we develop a class of efficient and accurate numerical schemes for general dissipative systems with global constraints. The schemes are based on the relaxed generalized SAV approach and the Lagrange multiplier approach, and enjoy many advantages such as solving only one linear system with constant coefficients and one nonlinear algebraic system for the Lagrange multipliers. Besides, the schemes preserve global constraints and are unconditionally energy stable with a modified energy, which is equal to the original energy in most cases. We present applications of the R-GSAV/LM approach to a variety of problems to demonstrate its effectiveness and advantages compared with existing approaches.

AMS subject classifications: 35Q40, 65M12, 35Q55, 65M70
Key words: SAV, dissipative system with global constraints, Lagrange multiplier, stability.

1. Introduction

Solutions for a large class of partial differential equations (PDEs) arising in physical, chemical, and biological sciences are not only energy dissipative, but also satisfy certain global constraints, such as preservation of norm, volume, surface area, etc. It is important to develop numerical schemes, which are energy dissipative and preserve these constraints at the discrete level.

While there are many different ways to design numerical schemes that are energy dissipative — cf. [11,13,19–23,26,27], there are relatively few approaches to preserve global constraints, among which the two popular ones are:

*Corresponding author. *Email addresses:* yanrongzhang_math@163.com (Y. Zhang), shen7@purdue.edu (J. Shen)

- **The penalty approach**. This approach is frequently used to deal with gradient flows with global constraints (cf. [7, 16, 18, 24, 27, 30]). The key is to add suitable penalty terms related to global constraints in the free energy of the underlying gradient flow. Then, one can apply usual methods for the new gradient flow with the augmented free energy. The drawback of this approach is that the problem may become very stiff as we increase the penalty strength to better preserve the constraints.

- **The Lagrange multiplier approach**. The main idea is to introduce Lagrange multipliers to enforce the global constraints (cf. [6, 12]). Although the Lagrange multiplier approach can in principle preserve the global constraints exactly, how to develop efficient, robust and energy stable numerical schemes for the system with Lagrange multipliers is still challenging. In [8], the authors proposed three numerical schemes for the Lagrange multiplier approach with different advantages and shortcomings. A particular issue is that the Lagrange multipliers are determined by solving a nonlinear algebraic system which may require exceedingly small time steps to have a suitable solution. This approach is also applied to nonlinear Schrödinger/Gross-Pitaevskii equations in [1] and Klein-Gordon Schrödinger (KGS) equations in [28]. It is found in [1] that, in some situations, the nonlinear algebraic system for the Lagrange multipliers may not admit a solution even at very small time steps.

In this paper, we propose a class of new schemes, referred hereafter to as the relaxed generalized SAV/Lagrange multiplier (R-GSAV/LM) approach, for general dissipative complex nonlinear systems with global constraints. This class of schemes combines the ideas and advantages of the relaxed generalized SAV (R-GSAV) approach [15, 17, 29] and the Lagrange multiplier approach [8]. More precisely, (i) the generalized SAV approach [15] is used to ensure unconditional stability with a modified energy; (ii) the Lagrange multiplier approach [8] is used to enforce the global constraints; and (iii) the relaxation idea in [17, 29] is used to improve the accuracy by relating the modified energy to the true energy. This class of schemes enjoys the following advantages: (i) it only requires solving one linear system with constant coefficients so it is very efficient; (ii) it can be higher-order accurate; (iii) it can preserve global constraints exactly by solving a nonlinear algebraic system for the Lagrange multipliers only, so it is much more robust as the Lagrange multipliers are decoupled from the SAV; (iv) it is unconditionally energy stable with a modified energy which, in most cases, equals to the original energy.

We apply our new schemes to several interesting models, including single-component and multi-component Bose Einstein Condensates (BECs), an optimal partition problem with multiple constraints, and Klein-Gordon-Schrödinger (KGS) equations.

The rest of this paper is organized as follows. In Section 2, we briefly review the Lagrange multiplier approaches in [8], and for the purpose of comparison, extend the second approaches in [8] to higher-order. In Section 3, we introduce our R-GSAV/LM approach for general dissipative systems, and derive a stability result. In Section 4, we apply our new schemes to imaginary time gradient flow of one- and multi-component BECs, optimal partition problem with multiple constraints, and KGS equations. Some concluding remarks are presented in Section 5.

2. A Brief Review of the Lagrange Multiplier Approach

We briefly review below the Lagrange multiplier approaches in [8] for gradient flows. Without loss of generality, we consider a gradient flow with total free energy in the form

$$E_{tot}(\phi)=\int_\Omega \frac{1}{2}\mathscr{L}\phi\cdot\phi+F(\phi)\mathrm{d}\boldsymbol{x},$$

under a global constraint

$$\frac{\mathrm{d}}{\mathrm{d}t}H(\phi)=0 \text{ with } H(\phi)=\int_\Omega h(\phi)\mathrm{d}\boldsymbol{x},$$

where $\mathscr{L}$ is a symmetric non-negative linear operator, and $H(\phi)$ is a function of ϕ. Then the gradient flow with the above constraint can be written as

$$\phi_t=-\mathscr{G}\mu, \tag{2.1}$$

$$\mu=\mathscr{L}\phi+F'(\phi)-\lambda(t)\frac{\delta H}{\delta\phi}, \tag{2.2}$$

$$\frac{\mathrm{d}}{\mathrm{d}t}H(\phi)=0, \tag{2.3}$$

where $\lambda(t)$ is a Lagrange multiplier introduced to enforce the constraint, and $\mathscr{G}$ is a symmetric positive definite operator describing the relaxation process. For example, $\mathscr{G}=I$ for the L^2 gradient flow and $\mathscr{G}=-\Delta$ for the H^{-1} gradient flow.

Taking the inner products of (2.1) with μ and of (2.2) with ϕ_t, summing up the results, we obtain the following energy dissipation law:

$$\frac{\mathrm{d}E_{tot}(\phi)}{\mathrm{d}t}=-(\mathscr{G}\mu,\mu)\le 0.$$

Three different numerical schemes for the above system were proposed in [8]. The first approach is the combination of the original SAV approach and Lagrange multiplier approach, which can preserve the global constraints exactly, but it is not necessarily unconditionally energy stable. The third approach is energy stable with the original energy but does not preserve global constraints exactly. The second approach is theoretically most attractive, which is unconditionally energy stable with the original energy and preserves the global constraints exactly, but it needs to solve a coupled nonlinear algebraic system for the Lagrange multipliers and the SAV at each time step. Hence, we shall only compare our new schemes with the second approach whose higher-order BDFk version takes the following form:

$$\frac{\alpha_k\phi^{n+1}-A_k(\phi^n)}{\delta t}=-\mathscr{G}\mu^{n+1}, \tag{2.4}$$

$$\mu^{n+1}=\mathscr{L}\phi^{n+1}+\eta^{n+1}F'\big(B_k(\phi^n)\big)-\lambda^{n+1}B_k\left(\left(\frac{\delta H}{\delta\phi}\right)^n\right), \tag{2.5}$$

$$H\left(\phi^{n+1}\right)=H\left(\phi^0\right), \tag{2.6}$$

$$\begin{aligned}&\int_\Omega \alpha_k F\left(\phi^{n+1}\right)-A_k\big(F(\phi^n)\big)\mathrm{d}\boldsymbol{x}\\&=\eta^{n+1}\left(F'\left(B_k\left(\phi^n\right)\right),\alpha_k\phi^{n+1}-A_k\left(\phi^n\right)\right)\\&\quad-\lambda^{n+1}\left(B_k\left(\left(\frac{\delta H}{\delta\phi}\right)^n\right),\alpha_k\phi^{n+1}-A_k\left(\phi^n\right)\right),\end{aligned}\tag{2.7}$$

where α_k, the operators A_k and B_k are given by

first-order:

$$\alpha_1=1,\quad A_1(\phi^n)=\phi^n,\quad B_1(\phi^n)=\phi^n,$$

second-order:

$$\alpha_2=\frac{3}{2},\quad A_2(\phi^n)=2\phi^n-\frac{1}{2}\phi^{n-1},\quad B_2(\phi^n)=2\phi^n-\phi^{n-1},$$

third-order:

$$\alpha_3=\frac{11}{6},\quad A_3\left(\phi^n\right)=3\phi^n-\frac{3}{2}\phi^{n-1}+\frac{1}{3}u^{n-2},\quad B_3\left(\phi^n\right)=3\phi^n-3\phi^{n-1}+\phi^{n-2},$$

and the formulae for $k=4,5,6$ can also be derived easily by Taylor expansion.

It can be easily shown [8] that the scheme (2.4)-(2.7) with $k=1,2$ is unconditionally energy stable in the sense that:

(i) For $k=1$, $E^{n+1}-E^n\le-\delta t(\mathscr{G}\mu^{n+1},\mu^{n+1})$, where

$$E^{n+1}=\frac{1}{2}\left(\mathscr{L}\phi^{n+1},\phi^{n+1}\right)+\int_\Omega F\left(\phi^{n+1}\right)\mathrm{d}\boldsymbol{x}.$$

(ii) For $k=2$, $\tilde{E}^{n+1}-\tilde{E}^n\le-\delta t(\mathscr{G}\mu^{n+1},\mu^{n+1})$, where

$$\begin{aligned}\tilde{E}^{n+1}=&\frac{1}{4}\left((\mathscr{L}\phi^{n+1},\phi^{n+1})+\left(\mathscr{L}(2\phi^{n+1}-\phi^n),2\phi^{n+1}-\phi^n\right)\right)\\&+\frac{1}{2}\int_\Omega 3F\left(\phi^{n+1}\right)-F\left(\phi^n\right)\mathrm{d}\boldsymbol{x}.\end{aligned}$$

3. The New R-GSAV/LM Approach

In this section, we describe a general framework to construct efficient numerical schemes for dissipative systems with global constraints. To fix the idea, we shall only consider a real-valued system with a single component and a single global constraint. Extensions to systems with multi-components and multi global constraints or with complex-valued solutions will be presented in the next section.

We consider the following general dissipative system

$$\frac{\partial\phi}{\partial t}+\mathscr{A}\phi+g(\phi)=\lambda(t)\frac{\delta H}{\delta\phi}\tag{3.1}$$

with a global constraint

$$\frac{\mathrm{d}}{\mathrm{d}t}H(\phi)=0 \quad \text{with} \quad H(\phi)=\int_{\Omega}h(\phi)\mathrm{d}\boldsymbol{x}, \tag{3.2}$$

where $\mathscr{A}$ is a positive definite operator, $g(\phi)$ is a semi-linear or quasi-linear operator, $\lambda(t)$ is a Lagrange multiplier introduced to enforce the constraint and $h(\phi)$ is a function of ϕ. We assume it satisfies an energy dissipation law as follows:

$$\frac{\mathrm{d}E_{tot}(\phi)}{\mathrm{d}t}=-\mathscr{K}(\phi), \tag{3.3}$$

where $E_{tot}(\phi)$ is a free energy with lower bound $-C_0$ and $\mathscr{K}(\phi)\geq 0$ for all ϕ.

The above system can come from constrained minimization problems, such as the gradient flow with constraint (2.1)-(2.3) where $\lambda(t)\neq 0$ is introduced to enforce the constraint (2.3), or from a dissipative system whose solution implicitly satisfies the constraint (3.2), e.g. the Klein-Gordon-Schrödinger equation considered in Subsection 4.3 below, where $\lambda(t)\equiv 0$ is introduced artificially to satisfy the constraint (3.2) at the discrete level.

Similar to [15], we set $E(\phi)=E_{tot}(\phi)+C_0$ and introduce a SAV $R(t)=E(\phi)$ to expand the Eqs. (3.1)-(3.3) into the following system:

$$\begin{aligned}
&\frac{\partial\phi}{\partial t}+\mathscr{A}\phi+g(\phi)=\lambda(t)\frac{\delta H}{\delta\phi},\\
&\frac{\mathrm{d}R(t)}{\mathrm{d}t}=-\frac{R(t)}{E(\phi)}\mathscr{K}(\phi),\\
&\frac{\mathrm{d}}{\mathrm{d}t}H(\phi)=0.
\end{aligned}$$

Then, we combine the ideas in [8, 15, 29] to construct the following relaxed generalized SAV/Lagrange multiplier (R-GSAV/LM) scheme: Given $(\phi^{n-k},R^{n-k}),\dots,(\phi^{n},R^{n})$, we compute (ϕ^{n+1},R^{n+1}) via the following three steps:

Step 1. Determine an intermediate solution $\widetilde{\phi}^{n+1}$, $\widetilde{R}^{n+1}$ by using the GSAV method

$$\frac{\alpha_k\bar{\phi}^{n+1}-A_k(\phi^n)}{\delta t}+\mathscr{A}\bar{\phi}^{n+1}+g\left[B_k(\phi^n)\right]=B_k\left(\lambda^n\left(\frac{\delta H}{\delta\phi}\right)^n\right), \tag{3.4}$$

$$\frac{1}{\delta t}\left(\widetilde{R}^{n+1}-R^n\right)=-\frac{\widetilde{R}^{n+1}}{E\left(\bar{\phi}^{n+1}\right)}\mathscr{K}\left(\bar{\phi}^{n+1}\right), \tag{3.5}$$

$$\xi_k^{n+1}=\frac{\widetilde{R}^{n+1}}{E(\bar{\phi}^{n+1})},\quad \eta_k^{n+1}=1-\left(1-\xi_k^{n+1}\right)^{k+1}, \tag{3.6}$$

$$\widetilde{\phi}^{n+1}=\eta_k^{n+1}\bar{\phi}^{n+1}. \tag{3.7}$$

Step 2. Find ϕ^{n+1} and λ^{n+1} from

$$\frac{\alpha_k(\phi^{n+1}-\widetilde{\phi}^{n+1})}{\delta t}=\lambda^{n+1}\left(\frac{\delta H}{\delta\phi}\right)^{n+1}-B_k\left(\lambda^n\left(\frac{\delta H}{\delta\phi}\right)^n\right), \tag{3.8}$$

$$H\left(\phi^{n+1}\right)=H\left(\phi^0\right). \tag{3.9}$$

Step 3. Update the SAV R^{n+1} via the following relaxation:

$$R^{n+1}=\zeta_0^{n+1}\widetilde{R}^{n+1}+\left(1-\zeta_0^{n+1}\right)E\left(\phi^{n+1}\right),\quad \zeta_0^{n+1}\in\mathscr{V}, \tag{3.10}$$

where

$$\mathscr{V}=\left\{\zeta\in[0,1]\ s.t.\ \frac{R^{n+1}-\widetilde{R}^{n+1}}{\delta t}=-\gamma^{n+1}\mathscr{K}\left(\phi^{n+1}\right)+\frac{\widetilde{R}^{n+1}}{E(\bar{\phi}^{n+1})}\mathscr{K}\left(\bar{\phi}^{n+1}\right)\right\} \tag{3.11}$$

with $\gamma^{n+1}\geq 0$ to be determined so that $\mathscr{V}$ is not empty.

The scheme (3.4)-(3.11) can be implemented as follows.

Algorithm 3.1

Solve $\bar{\phi}^{n+1}$ from (3.4).
Compute $\widetilde{R}^{n+1}$ from (3.5).
Compute ξ_k^{n+1} and η_k^{n+1} from (3.6).
Update $\widetilde{\phi}^{n+1}$ from (3.7).
Find $(\phi^{n+1},\lambda^{n+1})$ by solving the nonlinear algebraic system (3.8)-(3.9).
Update R^{n+1} by (3.10)-(3.11), and refer to [29] about how to choose ζ_0^{n+1} and γ^{n+1}. For the readers' convenience, we provide the choice of ζ_0^{n+1} and γ^{n+1} as below.
if $\tilde{R}^{n+1}=E(\phi^{n+1})$ **then**
    Set $\zeta_0^{n+1}=0$ and

$$\gamma^{n+1}=\frac{\tilde{R}^{n+1}\mathscr{K}(\bar{\phi}^{n+1})}{E(\bar{\phi}^{n+1})\mathscr{K}(\phi^{n+1})}.$$

end if
if $\tilde{R}^{n+1}>E(\phi^{n+1})$ **then**
    Set $\zeta_0^{n+1}=0$ and

$$\gamma^{n+1}=\frac{\tilde{R}^{n+1}-E(\phi^{n+1})}{\delta t\mathscr{K}(\phi^{n+1})}+\frac{\tilde{R}^{n+1}\mathscr{K}(\bar{\phi}^{n+1})}{E(\bar{\phi}^{n+1})\mathscr{K}(\phi^{n+1})}. \tag{3.12}$$

end if
if $\tilde{R}^{n+1}<E(\phi^{n+1})$ and $\tilde{R}^{n+1}-E(\phi^{n+1})+\delta t\frac{\tilde{R}^{n+1}}{E(\bar{\phi}^{n+1})}\mathscr{K}(\bar{\phi}^{n+1})\geq 0$ **then**
    Set $\zeta_0^{n+1}=0$ and γ^{n+1} the same as (3.12).
end if
if $\tilde{R}^{n+1}<E(\phi^{n+1})$ and $\tilde{R}^{n+1}-E(\phi^{n+1})+\delta t\frac{\tilde{R}^{n+1}}{E(\bar{\phi}^{n+1})}\mathscr{K}(\bar{\phi}^{n+1})<0$ **then**
    Set

$$\zeta_0^{n+1}=1-\frac{\delta t\tilde{R}^{n+1}\mathscr{K}(\bar{\phi}^{n+1})}{E(\bar{\phi}^{n+1})(E(\phi^{n+1})-\tilde{R}^{n+1})}$$

    and $\gamma^{n+1}=0$.
end if

Remark 3.1. If $h(\phi)=\phi^2$, which is the case for the applications we consider in this paper, the nonlinear algebraic equation (3.8)-(3.9) is quadratic about λ^{n+1} with two real roots given by $\lambda^{n+1}=(\alpha_k\pm\sqrt{s^{n+1}})/\delta t$ with

$$s^{n+1}=\int_\Omega\left|\alpha_k\widetilde{\phi}^{n+1}-\delta tB_k(\lambda^n\phi^n)\right|^2\mathrm{d}\boldsymbol{x}\Big/\int_\Omega|\phi_0|^2\mathrm{d}\boldsymbol{x}\geq 0.$$

We should choose the root with smaller absolute value, namely,

$$\lambda^{n+1}=\frac{1}{\delta t}\left(\alpha_k-\sqrt{s^{n+1}}\right).$$

Remark 3.2. Similar to the ideas [9,10,14], we can use the $(k-1)$-th order extrapolation of the Lagrange multiplier term in (3.4) and (3.8). In such a way, scheme (3.4)-(3.11) is still k-th order accuracy.

Theorem 3.1. *Given $R^n\geq 0$, we have $R^{n+1}\geq 0$, $\xi_k^{n+1}\geq 0$, and the scheme* (3.4)-(3.11) *for any k is unconditionally energy stable in the sense that*

$$R^{n+1}-R^n=-\delta t\gamma^{n+1}\mathscr{K}(\phi^{n+1})\leq 0. \tag{3.13}$$

Furthermore, if $E(\phi)=(\mathscr{L}\phi,\phi)/2+E_1(\phi)$ with $\mathscr{L}$ being a linear positive definite operator and $E_1(\phi)$ bounded from below, then there exists $C_0>0$ such that

$$\left(\mathscr{L}\tilde{\phi}^n,\tilde{\phi}^n\right)\leq C_0 \tag{3.14}$$

for all n.

Proof. The proof is essentially the same as the proof of [15, Theorem 1]. Since $E(\bar{\phi}^{n+1})>0$, the relation (3.5) yields that for a given $R^n\geq 0$ we have

$$\widetilde{R}^{n+1}=\frac{R^n}{1+\delta t.\mathscr{K}(\bar{\phi}^{n+1})/E(\bar{\phi}^{n+1})}\geq 0. \tag{3.15}$$

Then we derive from (3.6) that $\xi_k^{n+1}\geq 0$, and we derive from (3.10) that $R^{n+1}\geq 0$. Combining (3.5) and (3.11), we obtain (3.13). Denoting $M:=R^0=E[\phi(\cdot,0)]$, we derive from (3.13) and (3.15) that $\widetilde{R}^{n+1}\leq M$ for all n.

Without loss of generality, we can assume $E_1(\phi)>1$ for all ϕ. It then follows from (3.6) that

$$\left|\xi_k^{n+1}\right|=\frac{\widetilde{R}^{n+1}}{E(\bar{\phi}^{n+1})}\leq\frac{2M}{(\mathscr{L}\bar{\phi}^{n+1},\bar{\phi}^{n+1})+2}. \tag{3.16}$$

Then

$$\eta_k^{n+1}=1-\left(1-\xi_k^{n+1}\right)^{k+1}=\xi_k^{n+1}P_k\left(\xi_k^{n+1}\right)$$

with P_k being a polynomial of degree k. We derive from (3.16) that there exists $M_k>0$ such that

$$\left|\eta_k^{n+1}\right|=\left|\xi_k^{n+1}P_k\left(\xi_k^{n+1}\right)\right|\leq\frac{M_k}{(\mathscr{L}\bar{\phi}^{n+1},\bar{\phi}^{n+1})+2},$$

which, along with $\widetilde{\phi}^{n+1} = \eta_k^{n+1}\bar{\phi}^{n+1}$, implies

$$\begin{aligned}\left(\mathscr{L}\widetilde{\phi}^{n+1}, \widetilde{\phi}^{n+1}\right) &= \left(\eta_k^{n+1}\right)^2 \left(\mathscr{L}\bar{\phi}^{n+1}, \bar{\phi}^{n+1}\right) \\ &\leq \left(\frac{M_k}{(\mathscr{L}\bar{\phi}^{n+1}, \bar{\phi}^{n+1}) + 2}\right)^2 \left(\mathscr{L}\bar{\phi}^{n+1}, \bar{\phi}^{n+1}\right) \leq M_k^2. \qquad \square\end{aligned}$$

Remark 3.3. The scheme (3.4)-(3.11) is very efficient as it only requires solving one linear system with constant coefficients in (3.4). Besides, it also preserve the global constraint exactly.

We are unable to prove $(\mathscr{L}\phi^{n+1}, \phi^{n+1}) \leq C_0$ due to the nonlinear nature of (3.9). But since $\tilde{\phi}^{n+1}$ is also a k-th order approximation of $\phi(\cdot, t_{n+1})$, the bound $(\mathscr{L}\tilde{\phi}^{n+1}, \tilde{\phi}^{n+1}) \leq C_0$ will still be useful in the error analysis that is under investigation.

4. Applications

We present in this section ample applications to validate the efficiency and accuracy of the R-GSAV/LM scheme (3.4)-(3.11), with comparisons to the Lagrange multiplier (LM) approach (2.4)-(2.7), and the modified SAV (MSAV) schemes with penalization proposed in [30].

Unless specified otherwise, we consider examples with periodic boundary condition and use the Fourier-spectral method for spatial discretization so that all the linear systems in our time discretization schemes can be solved very efficiently by using the fast Fourier transform.

4.1. Computing ground state solutions via imaginary time gradient flows

In this subsection, we use our R-GSAV/LM scheme to compute ground state solutions of one- and multi-component BECs through solving the imaginary time gradient flows.

4.1.1. One-component BECs

We first consider the one-component BEC system with the free energy

$$E_{tot}(\phi) = \frac{1}{2}(\phi, \mathscr{L}\phi) + \frac{1}{2}\int_\Omega F\left(|\phi|^2\right) \mathrm{d}\boldsymbol{x}, \tag{4.1}$$

subject to the constraint

$$H(\phi) := \int_\Omega |\phi(\boldsymbol{x}, t)|^2 \mathrm{d}\boldsymbol{x} = 1, \tag{4.2}$$

where $F(\phi)$ is a nonlinear potential function — e.g. $F(\phi) = (\beta/2)\phi^2$, and $\mathscr{L}$ is a positive definite operator: $\mathscr{L}\phi = (-(1/2)\Delta + V(x))\phi$ with $V(x) \geq 0$.

Since the ground states of one-component BECs are the minimizers of free energy (4.1), a popular approach to find the ground state solutions is to seek the steady state solution of an imaginary time gradient flow [3]. Previously, the constraint (4.2) in the imaginary time gradient flow was handled either with a projection approach [3] or a penalty approach [30]. We shall adopt the Lagrange multiplier approach. More precisely, we introduce a Lagrange multiplier $\lambda(t)$ to enforce (4.2), and consider the following imaginary time gradient flow with a Lagrange multiplier:

$$\begin{aligned}
\phi_t &= -\frac{\delta E_{tot}(\phi)}{\delta \phi} + \frac{\delta H(\phi)}{\delta \phi} \\
&= -\mathscr{L}\phi - F'\left(|\phi|^2\right)\phi - \lambda(t)\phi, \quad \boldsymbol{x} \in \Omega, \quad t > 0, \\
&\lim_{|\boldsymbol{x}|\to\infty} \phi(\boldsymbol{x}, t) = 0, \quad t \geq 0, \\
&H(\phi) = 1, \qquad\qquad t \geq 0.
\end{aligned}$$

It is easy to see that the system satisfies the following energy dissipative law:

$$\frac{\mathrm{d}E_{tot}(\phi)}{\mathrm{d}t} = -\left\|\mathscr{L}\phi + F'\left(|\phi|^2\right)\phi + \lambda(t)\phi\right\|^2 \leq 0.$$

Therefore, we can directly apply the scheme (3.4)-(3.11) to the above system.

We impose BECs with the periodic boundary condition, and always compute on a domain, which is large enough such that the periodic boundary condition do not introduce a significant truncation error.

Example 4.1. We first test the accuracy in time for the first- and second-order R-GSAV/LM schemes by considering the following initial condition:

$$V(x) = \frac{x^2}{2}, \quad \beta = 60, \quad \phi_0(x) = \frac{e^{-x^2/2}}{(\pi)^{1/4}} \tag{4.3}$$

in $\Omega = (-8, 8)$. We use 128 modes for space discretization so that the spatial discretization error is negligible when compared with the time discretization error. The error is computed at $T = 0.1$, with the reference solution computed using the time step $\delta t = 10^{-6}$. We plot the L^2 error in Fig. 1, where we can observe the first-order and second-order accuracy.

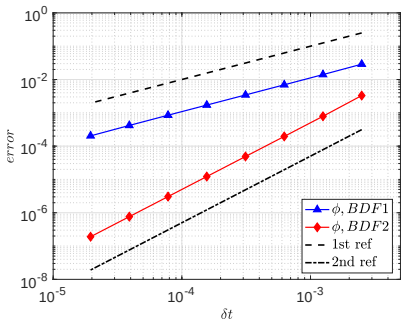

Figure 1: Example 4.1. Accuracy of the first-order and second-order schemes for one-component BECs.

Example 4.2. In this example, we examine the efficiency of the schemes for computing ground state of BECs. Still considering the initial condition (4.3), we compare the iteration number K and energy $E_\beta(\phi) = 2E_{tot}(\phi)$ between the modified SAV (MSAV) schemes with penalization proposed in [30], the LM schemes and the R-GSAV/LM schemes. The stopping criterion for the steady state solution is $|E_\beta(\phi^{n+1}) - E_\beta(\phi^n)| < 10^{-6}$. We are concerned about how to use a larger time step and less iterative numbers to obtain accurate results, therefore the time step we use here is $\delta t = 10^{-2}$. The computational results of the MSAV, LM and R-GSAV/LM approaches are summarized in Table 1. It can be observed that the R-GSAV/LM approach requires fewer iterations than MSAV approach and LM approach, especially for BDF1 scheme. In addition, the computational cost of the R-GSAV/LM approach at each time step is lower than the MSAV and LM approaches, thus, the R-GSAV/LM approach are more competitive compared with MSAV and LM schemes for this example.

Table 1: Example 4.2. Iteration numbers and energies based on three different approaches with $\delta t = 10^{-2}$ for one-component BECs in 1D.

	K(BDF1)	E_β(BDF1)	K(BDF2)	E_β(BDF2)
MSAV	195	6.075956	180	6.075955
LM	191	6.075956	180	6.075956
R-GSAV/LM	175	6.075955	178	6.075956

Example 4.3. In this example, we compute the ground state solution in two-dimensions. The initial condition is chosen as

$$\phi_0(x,y) = \frac{(\gamma_x\gamma_y)^{1/4}}{\pi^{1/2}} e^{-(\gamma_x x^2 + \gamma_y y^2)/2}$$

with two different potential functions.

Case 1. A harmonic oscillator potential

$$V(x,y) = \frac{1}{2}\left(\gamma_x^2 x^2 + \gamma_y^2 y^2\right).$$

Case 2. A harmonic oscillator potential plus a potential of a stirrer corresponding to a far-blue detuned Gaussian laser beam which is used to generate vortices in BECs

$$V(x,y) = \frac{1}{2}\left(\gamma_x^2 x^2 + \gamma_y^2 y^2\right) + \omega_0 e^{-\delta((x-r_0)^2+y^2)}.$$

The parameters are chosen as $\gamma_x = 1, \gamma_y = 4$ and $\beta = 200$ in Case 1 and $\gamma_x = 1, \gamma_y = 1, \omega_0 = 4, \delta = r_0 = 1$, and $\beta = 200$ in Case 2. We then solve Case 1 on $\Omega_1 = [-8,8] \times [-4,4]$ and Case 2 on $\Omega_2 = [-8,8] \times [-8,8]$. In both cases, we chose 128^2 Fourier modes, and used the first-order R-GSAV/LM scheme with $\delta t = 10^{-3}$.

The chemical potential and the energy of the ground state are listed in Table 2, where

$$x_{\rm rms} = \|x\phi\|_{L^2(\Omega)}, \quad y_{\rm rms} = \|y\phi\|_{L^2(\Omega)},$$

and $\mu_g = \mu_\beta(\phi_g)$ with

$$\begin{aligned}\mu_\beta(\phi) &= \int_\Omega \left(\frac{1}{2}|\nabla\phi(x)|^2 + V(x)|\phi(x)|^2 + \beta|\phi(x)|^4\right)\mathrm{d}\boldsymbol{x} \\ &= E_\beta(\phi) + \int_\Omega \frac{\beta}{2}|\phi(x)|^4\mathrm{d}\boldsymbol{x}.\end{aligned}$$

We observe from the Table 2 that the results by our R-GSAV/LM approach are consistent with the results obtained by the TSSP method [3], the modified SAV method [30] and the generalized multiple SAV approach [16].

Table 2: Example 4.3. The chemical potential and the energy of ground state in 2D.

	x_{rms}	y_{rms}	$E_\beta(\phi_g)$	μ_g
Case 1	2.2767	0.6100	11.1562	16.3068
Case 2	1.6945	1.7137	5.8507	8.3280

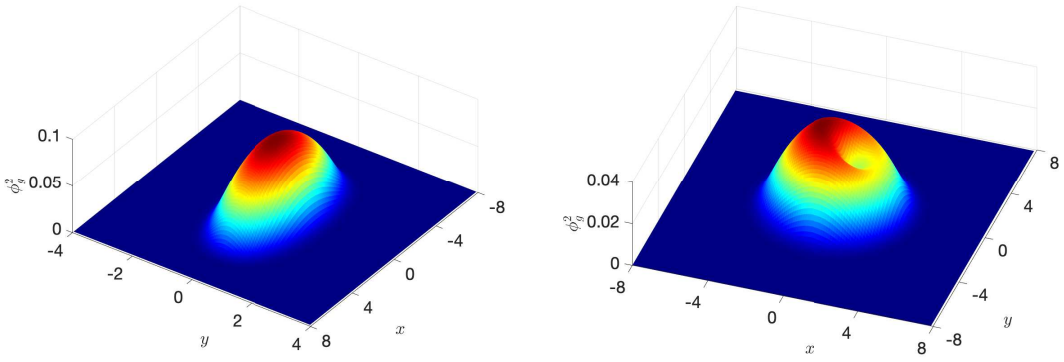

Figure 2: Example 4.3. Ground state solutions for BECs in the 2D.

4.1.2. Two-component BECs

Here we consider two-component BECs with the free energy [2, 25] given by

$$\begin{aligned}&E_{tot}(\phi_1, \phi_2) \\ &= \int_\Omega \left(\frac{1}{2}|\nabla\phi_1|^2 + \frac{1}{2}|\nabla\phi_2|^2\right) + V_1(x)|\phi_1|^2 + V_2(x)|\phi_2|^2\mathrm{d}\boldsymbol{x} + E_0(\phi_1, \phi_2),\end{aligned}$$

where

$$E_0(\phi_1,\phi_2)$$
$$=\int_\Omega\left[\frac{1}{2}\beta_{11}|\phi_1|^4+\frac{1}{2}\beta_{22}|\phi_2|^4+\beta_{12}|\phi_1|^2|\phi_2|^2+\rho\phi_1\phi_2+\frac{\delta}{2}\left(|\phi_1|^2-|\phi_2|^2\right)\right]\mathrm{d}\boldsymbol{x},$$

subject to the constraint

$$\int_\Omega|\phi_1(x,t)|^2\mathrm{d}\boldsymbol{x}+\int_\Omega|\phi_2(x,t)|^2\mathrm{d}\boldsymbol{x}=1,\quad t\geq 0. \tag{4.4}$$

The unknown functions ϕ_1,ϕ_2 are the macroscopic wave function corresponding to the spin-up and spin-down components, $V_i(x)$ $(i=1,2)$ are two external trapping potentials, ρ is the effective Rabi frequency, δ is the Raman transition constant, β_{ij} $(i,j=1,2)$ are related to the s-wave scattering lengths between i-th and j-th components (positive for repulsive interaction and negative for attractive interaction).

Introducing a Lagrange multiplier $\lambda(t)$ to enforce (4.4), the solution of the constrained minimization problem can be cast as the steady state solution of the following imaginary time gradient flow:

$$\frac{\partial\phi_1}{\partial t}=\left(\frac{1}{2}\Delta-V_1(x)-\frac{\delta}{2}-\left(\beta_{11}|\phi_1|^2+\beta_{12}|\phi_2|^2\right)\right)\phi_1$$
$$-\frac{\rho}{2}\phi_2+\lambda(t)\phi_1,\qquad \boldsymbol{x}\in\Omega,\quad t>0, \tag{4.5}$$
$$\frac{\partial\phi_2}{\partial t}=\left(\frac{1}{2}\Delta-V_2(x)+\frac{\delta}{2}-\left(\beta_{12}|\phi_1|^2+\beta_{22}|\phi_2|^2\right)\right)\phi_2$$
$$-\frac{\rho}{2}\phi_1+\lambda(t)\phi_2,\qquad \boldsymbol{x}\in\Omega,\quad t>0, \tag{4.6}$$
$$\int_\Omega|\phi_1(x,t)|^2\mathrm{d}\boldsymbol{x}+\int_\Omega|\phi_2(x,t)|^2\mathrm{d}\boldsymbol{x}=1,\quad t\geq 0. \tag{4.7}$$

Then, we can construct a R-GSAV/LM scheme similar to (3.4)-(3.11) for the above system. The main difference is that we need to replace the single equation (3.4) to two equations corresponding to (4.5)-(4.6).

Example 4.4. We first compute the ground state solution. Set $V_1(x)=V_2(x)=x^2/2,\sigma=0$ and $\beta_{11}:\beta_{12}:\beta_{22}=(1:0.94:0.97)\beta$ with β to be given. The initial condition are chosen as

$$\phi_1^0(x)=\phi_2^0(x)=\frac{1}{\pi^{1/4}\sqrt{2}}e^{-x^2/2}.$$

First, we summarized in Table 3 the required iteration numbers to reach the steady state, and the energy at the steady state with $\delta t=10^{-2}$, $\beta=100$ and $\rho=-2$ computed by the MSAV, LM and R-GSAV/LM approaches. The stopping criterion for the steady state solution is

$$\left|E_{tot}(\phi^{n+1})-E_{tot}(\phi^n)\right|<10^{-6}.$$

Table 3: Example 4.4. Iteration numbers and energies with $\delta t = 10^{-2}$ based on three different approaches for the case $\beta = 100$ and $\rho = -2$ for two-component BECs in 1D.

	K(BDF1)	E(BDF1)	K(BDF2)	E(BDF2)
MSAV	196	7.293210	176	7.293208
LM	190	7.293211	-	-
R-GSAV/LM	170	7.293210	174	7.293211

We observe from this table that the R-GSAV/LM approach is also very efficient for computing the ground state solution of the two-component BECs. Note that for the Newton iteration in the second-order LM approach does not converge with $\delta t = 10^{-2}$, a smaller time step is needed.

Next, we show that the relaxation step — i.e. the Step 3 of R-GSAV/LM approach, can indeed improve the accuracy and robustness. For the sake of comparison, we refer the R-GSAV/LM scheme without the relaxation step as the GSAV/LM scheme. We plot in Figs. 3 and 4 solutions and the energy evolution computed by first-order GSAV/LM and R-GSAV/LM schemes with $\delta t = 10^{-2}$ along with the reference solution obtained by the first-order LM scheme with $\delta t = 10^{-4}$ for the case $\beta = 100$ and $\rho = -2$. We observe that the solution computed by the GSAV/LM scheme is totally wrong while the solution by the R-GSAV/LM scheme is indistinguishable with the reference solution. We also plot the

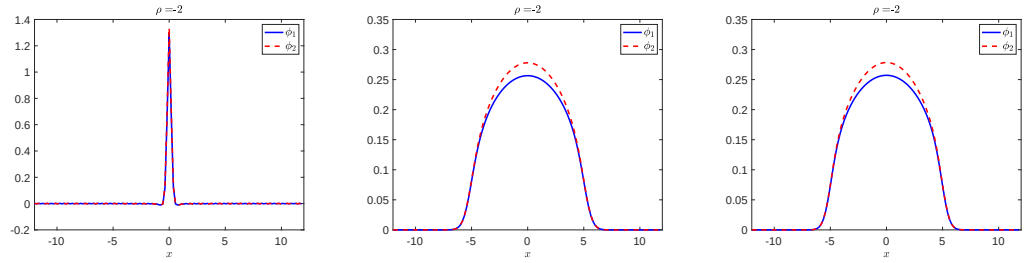

Figure 3: Example 4.4. Steady state solution of two-component BECs determined by different methods. Left: First-order GSAV/LM scheme. Middle: First-order R-GSAV/LM scheme. Right: Reference solution.

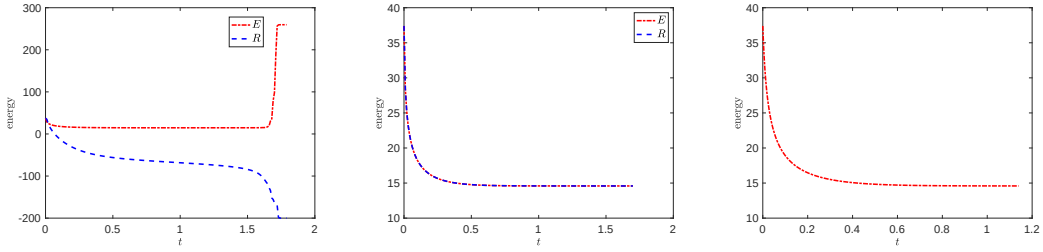

Figure 4: Example 4.4. Evolution of energy of two-component BECs determined by different methods. Left: First-order GSAV/LM scheme. Middle: First-order R-GSAV/LM scheme. Right: Reference solution.

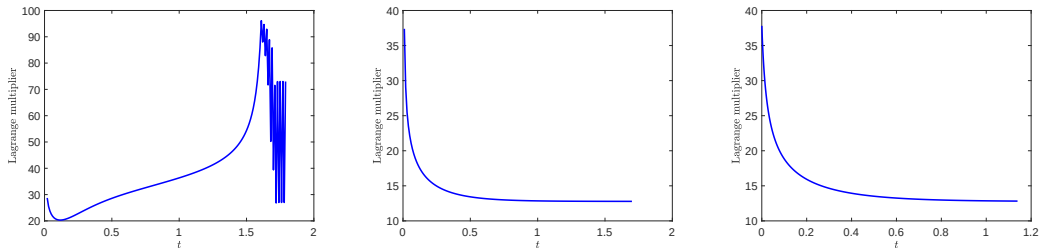

Figure 5: Example 4.4. Evolution of Lagrange multiplier of two-component BECs determined by different methods. Left: First-order GSAV/LM scheme. Middle: First-order R-GSAV/LM scheme. Right: Reference solution.

corresponding evolution of the Lagrange multipliers in Fig. 5. These figures indicate that the R-GSAV/LM scheme is much more accurate and robust at larger time steps.

4.2. Application to an optimal partition model

We consider an optimal partition problem which is a multicomponent system with multiple constraints.

Given a positive integer m and a small parameter ϵ, the total free energy is given by

$$E_{tot}(\boldsymbol{\phi}) = \int_\Omega \left(\frac{1}{2}|\nabla \boldsymbol{\phi}|^2 + \boldsymbol{F}(\boldsymbol{\phi})\right) \mathrm{d}\boldsymbol{x},$$

where $\boldsymbol{\phi} \in \mathbb{X}^m$ ($\mathbb{X} \subset H^1(\Omega)$ with suitable boundary conditions) is a vector valued function satisfying the norm constraints

$$H_j(\phi_j) := \int_\Omega |\phi_j|^2 \mathrm{d}\boldsymbol{x} = 1, \quad j = 1, 2, \ldots, m, \tag{4.8}$$

$\boldsymbol{F}$ represents interaction potential of each partition

$$\boldsymbol{F}(\boldsymbol{\phi}) = \frac{1}{\epsilon^2} \sum_{i=2}^{m} \sum_{j<i} \phi_i^2 \phi_j^2.$$

We introduce m Lagrange multipliers $\{\lambda_j(t)\}_{j=1}^m$ to enforce the norm constraints (4.8). Then, the solution of the above constrained minimization problem can be cast as the steady state solutions of the following imaginary time gradient system:

$$\partial_t \phi_j = -M\mu_j, \qquad j = 1, 2, \ldots, m, \tag{4.9}$$

$$\mu_j = -\Delta \phi_j + \frac{\delta \boldsymbol{F}}{\delta \phi_j} - \lambda_j(t)\phi_j, \quad j = 1, 2, \ldots, m, \tag{4.10}$$

$$\frac{\mathrm{d}}{\mathrm{d}t} H_j(\phi_j) = 0, \qquad j = 1, 2, \ldots, m \tag{4.11}$$

with periodic or homogeneous Neumann boundary conditions, where $M > 0$ is a mobility constant.

Taking the inner products of (4.9) with μ_j and of (4.10) with $\partial_t\phi_j, j=1,2,\dots,m$, noticing the equality (4.11) and integrating by parts, we obtain the following energy dissipative law:

$$\frac{\mathrm{d}}{\mathrm{d}t}E_{tot}(\boldsymbol{\phi})=-M\int_\Omega\sum_{j=1}^m\mu_j^2\mathrm{d}\boldsymbol{x}. \tag{4.12}$$

Similar to (3.4)-(3.11), we can construct a R-GSAV/LM scheme for the above system. More exactly, for a given $(\boldsymbol{\phi}^{n-k},\mu^{n-k},R^{n-k}),\dots,(\boldsymbol{\phi}^n,\mu^n,R^n)$, we compute $(\boldsymbol{\phi}^{n+1},\mu^{n+1},R^{n+1})$ as follows:

Step 1. Determine an intermediate solution $\widetilde{\boldsymbol{\phi}}^{n+1}$, $\widetilde{\mu}^{n+1}$, $\widetilde{R}^{n+1}$ by using the GSAV method

$$\frac{\alpha_k\bar{\phi}_j^{n+1}-A_k\left(\phi_j^n\right)}{\delta t}=-M\widetilde{\mu}_j^{n+1}, \qquad j=1,\dots,m, \tag{4.13}$$

$$\widetilde{\mu}_j^{n+1}=-\Delta\bar{\phi}_j^{n+1}+B_k\left[\left(\frac{\delta\boldsymbol{F}}{\delta\phi_j}\right)^n-\lambda_j^n\phi_j^n\right], \qquad j=1,\dots,m, \tag{4.14}$$

$$\bar{\mu}_j^{n+1}=-\Delta\bar{\phi}_j^{n+1}+\frac{\delta\boldsymbol{F}}{\delta\phi_j}\left(\bar{\boldsymbol{\phi}}^{n+1}\right)-\lambda_j^n\bar{\phi}_j^{n+1}, \qquad j=1,\dots,m, \tag{4.15}$$

$$\frac{1}{\delta t}\left(\widetilde{R}^{n+1}-R^n\right)=-\frac{\widetilde{R}^{n+1}}{E(\bar{\boldsymbol{\phi}}^{n+1})}M\int_\Omega\sum_{j=1}^m\left(\bar{\mu}_j^{n+1}\right)^2\mathrm{d}\boldsymbol{x}, \tag{4.16}$$

$$\xi_k^{n+1}=\frac{\widetilde{R}^{n+1}}{E(\bar{\boldsymbol{\phi}}^{n+1})},\quad \eta_k^{n+1}=1-\left(1-\xi_k^{n+1}\right)^{k+1}, \tag{4.17}$$

$$\widetilde{\phi}_j^{n+1}=\eta_k^{n+1}\bar{\phi}_j^{n+1}, \qquad j=1,\dots,m. \tag{4.18}$$

Step 2. Find $\boldsymbol{\phi}^{n+1}$ and λ^{n+1} from

$$\frac{\alpha_k(\phi_j^{n+1}-\widetilde{\phi}_j^{n+1})}{\delta t}=M\lambda_j^{n+1}\phi_j^{n+1}-MB_k\left(\lambda_j^n\phi_j^n\right), \quad j=1,\dots,m, \tag{4.19}$$

$$H_j\left(\phi_j^{n+1}\right)=H_j\left(\phi_j^0\right), \qquad j=1,\dots,m. \tag{4.20}$$

Step 3. Update R^{n+1} via the following relaxation:

$$R^{n+1}=\zeta_0^{n+1}\widetilde{R}^{n+1}+\left(1-\zeta_0^{n+1}\right)E_{tot}\left(\boldsymbol{\phi}^{n+1}\right),\quad \zeta_0^{n+1}\in\mathscr{V}, \tag{4.21}$$

where

$$\mathscr{V}=\left\{\zeta\in[0,1]\ s.t.\ \frac{R^{n+1}-\widetilde{R}^{n+1}}{\delta t}=-\gamma^{n+1}M\int_\Omega\sum_{j=1}^m\left(\mu_j^{n+1}\right)^2\mathrm{d}\boldsymbol{x}+\frac{\widetilde{R}^{n+1}}{E(\bar{\boldsymbol{\phi}}^{n+1})}M\int_\Omega\sum_{j=1}^m\left(\bar{\mu}_j^{n+1}\right)^2\mathrm{d}\boldsymbol{x}\right\} \tag{4.22}$$

with

$$\mu_j^{n+1} = -\Delta\phi_j^{n+1} + \frac{\delta \boldsymbol{F}}{\delta \phi_j}\left(\boldsymbol{\phi}^{n+1}\right) - \lambda_j^{n+1}\phi_j^{n+1}, \quad j = 1, 2, \ldots, m,$$

and $\gamma^{n+1} \geq 0$ to be determined so that $\mathscr{V}$ is not empty.

We can establish a stability result similar to Theorem 3.1 for the above scheme, which can also be efficiently implemented similarly as the scheme (3.4)-(3.11).

We present below some numerical experiments for the optimal partition problem. We set $\Omega = [-\pi, \pi]^2$, and use 128^2 Fourier modes with $\varepsilon = 0.01$ in all following computations. To better visualize the subdomain evolution, we set the initial condition ϕ_i to be the marker function χ_i, which equals to 1 in the region i, and $\chi_i = 0$ in other region. The second-order R-GSAV/LM scheme with time step $\delta t = 10^{-5}$ is used.

Example 4.5. First, we take $m = 4$ with four connected trapezoids as the initial condition. Fig. 6 depict the evolutions of the phase configuration at $T = 0, 0.05, 0.5, 1, 5, 10$. It shows that patterns in the partition eventually evolve into hexagonal patterns.

We also plot the evolutions of Lagrange multipliers $\lambda_1, \lambda_2, \lambda_3$ and λ_4 in Fig. 7, which are positive and decay with time. These results are in agreement with [5, 8].

Fig. 8 presents the evolutions of modified energy $R(t), \zeta_0^{n+1}$ and errors of global constraints. We observe in particular that ζ_0^{n+1} remain to be 0, which means that the modified energy equals to the original energy.

We remark that if we use the LM scheme to simulate this example, a much smaller time step needs to be used. This is due to the fact that in the LM approach, the Lagrange multipliers for the constraints and for the energy dissipation are coupled together, making the nonlinear algebraic system more difficult to solve. In fact, for this example, we need $\delta t = 10^{-7}$ to get the correct solution with the LM scheme, while we can use $\delta t = 10^{-5}$ with the R-GSAV/LM scheme.

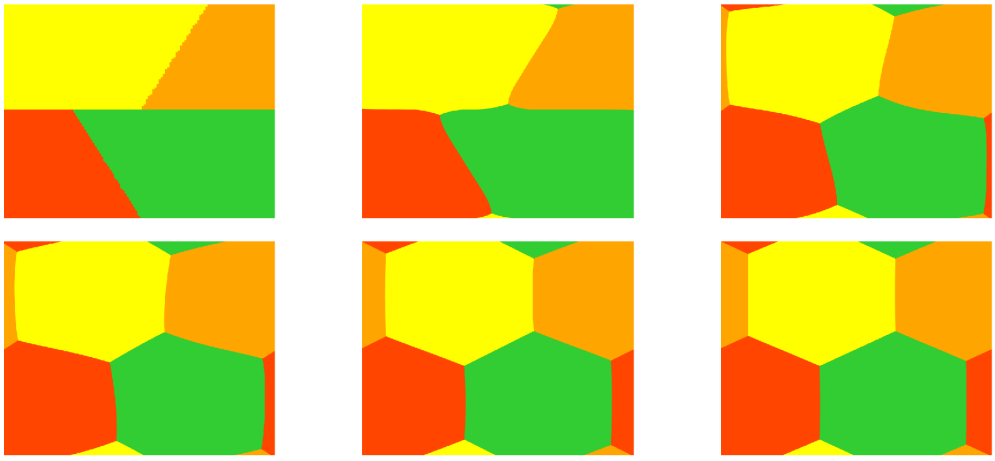

Figure 6: Example 4.5. A 4-subdomain partition: initial partition and subdomains at times $T = 0, 0.05, 0.5, 1, 5, 10$ computed by the second-order R-GSAV/LM scheme.

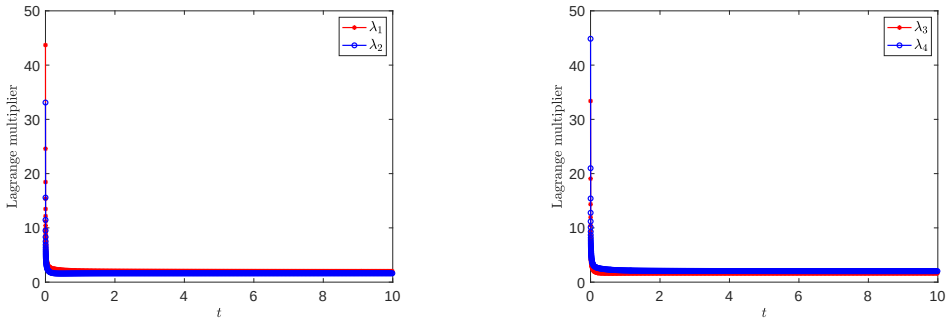

Figure 7: Example 4.5. Evolution of Lagrange multipliers $\lambda_1, \lambda_2, \lambda_3$ and λ_4 for four-subdomain partition in Fig. 6.

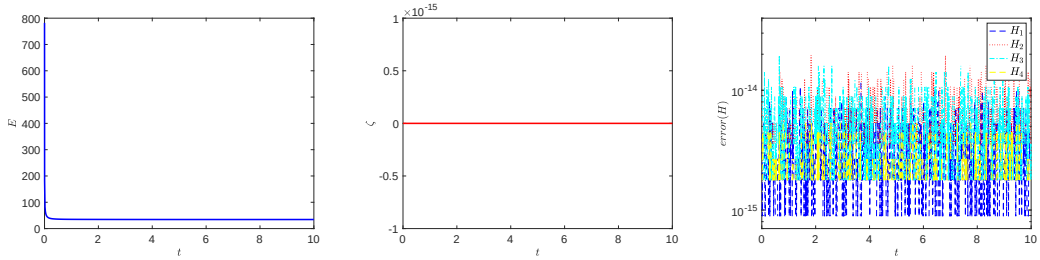

Figure 8: Example 4.5. Four-subdomain partition. Left: Evolution of energy. Middle: ζ_0^{n+1}. Right: Errors of global constraints.

Example 4.6. To further demonstrate the robustness of our R-GSAV/LM approach, we also simulate the case with $m = 10$ and plot the results in Fig. 9 which are consistent with those reported in [8, 12].

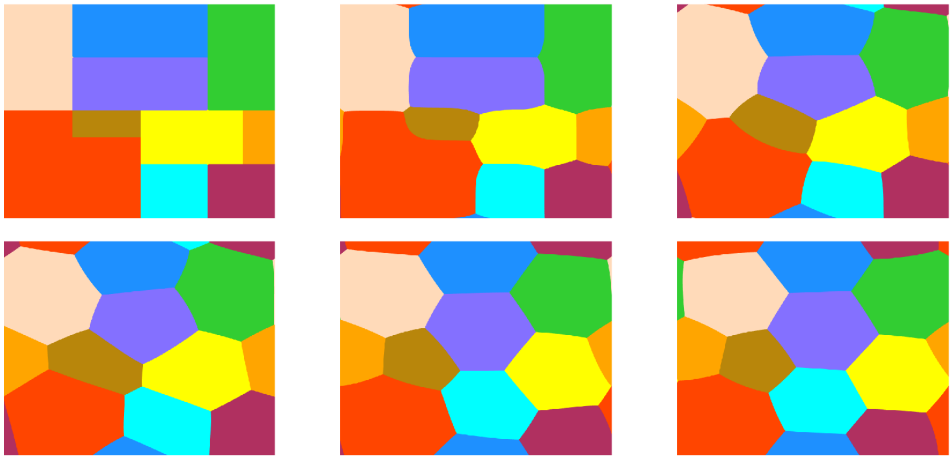

Figure 9: Example 4.6. A 10-subdomain partition: Initial partition and subdomains at time $T = 0, 0.05, 0.5, 2, 5, 10$ computed by the second-order R-GSAV/LM scheme.

4.3. Application to Klein-Gordon-Schrödinger equations

We consider the following Klein-Gordon-Schrödinger (KGS) equations:

$$\mathrm{i}\partial_t\psi + \Delta\psi + \phi\psi = 0, \qquad \boldsymbol{x}\in\Omega, \quad t>0, \tag{4.23}$$

$$\varepsilon^2\partial_{tt}\phi + \rho\varepsilon\partial_t\phi - \Delta\phi + \phi - |\psi|^2 = 0, \qquad \boldsymbol{x}\in\Omega, \quad t>0, \tag{4.24}$$

$$\psi(\boldsymbol{x},0)=\psi^{(0)}(\boldsymbol{x}), \quad \phi(\boldsymbol{x},0)=\phi^{(0)}(\boldsymbol{x}), \quad \partial_t\phi(\boldsymbol{x},0)=\phi^{(1)}(\boldsymbol{x}), \quad \boldsymbol{x}\in\Omega, \tag{4.25}$$

where Ω is a bounded domain in $\mathbb{R}^d$, $d=1,2,3$, and unknown function ψ and ϕ are prescribed with either homogeneous Dirichlet or periodic boundary conditions. In the above, the complex-valued function $\psi=\psi(\boldsymbol{x},t)$ represents a scalar nucleon field, the real-valued function $\phi=\phi(\boldsymbol{x},t)$ represents a scalar meson field, $\varepsilon>0$ is a parameter inversely proportional to the speed of light, and ρ is a nonnegative parameter.

The above KGS equations enjoy the following two properties:

(i) Energy dissipative law: If $\rho>0$, then

$$\frac{\mathrm{d}E_{tot}(t)}{\mathrm{d}t} = -\rho\varepsilon\int_\Omega |\partial_t\phi|^2\,\mathrm{d}\boldsymbol{x} \leqslant 0, \quad t\geqslant 0,$$

where

$$E_{tot}(t) = \int_\Omega \left[\frac{1}{2}\left(\phi^2+\varepsilon^2(\partial_t\phi)^2+|\nabla\phi|^2\right)+|\nabla\psi|^2-|\psi|^2\phi\right]\mathrm{d}\boldsymbol{x}.$$

(ii) Conservation of wave energy:

$$\frac{\mathrm{d}H(\psi)}{\mathrm{d}t}=0,$$

where

$$H(\psi) := \int_\Omega |\psi|^2\mathrm{d}\boldsymbol{x}.$$

We need to introduce a Lagrange multiplier $\lambda(t)$ to enforce the conservation of wave energy at the discrete level. Since $\lambda(t)\equiv 0$ at the continuous level and the solution is a complex-valued function, it is not clear whether we should introduce a real or imaginary $\lambda(t)$. We can determine which choice is suitable by considering the simple linear Schrödinger equation

$$\mathrm{i}\partial_t\psi = -\Delta\psi, \tag{4.26}$$

which also conserves the wave energy — i.e. $\mathrm{d}H(\psi)/\mathrm{d}t=0$. Setting $\psi=u+\mathrm{i}v$ with u and v being real functions, we can rewrite (4.26) as

$$\partial_t u = -\Delta v, \quad \partial_t v = \Delta u.$$

Then, we can introduce a real Lagrange multiplier $\lambda(t)$ to enforce $\mathrm{d}H(\psi)/\mathrm{d}t=0$ as follows:

$$\partial_t u = -\Delta v + \lambda\frac{\delta H}{\delta u} = -\Delta v + \lambda u,$$

$$\partial_t v = \Delta u + \lambda \frac{\delta H}{\delta v} = \Delta u + \lambda v,$$
$$\frac{\mathrm{d}H(\psi)}{\mathrm{d}t} = 0,$$

which can be rewritten as

$$\mathrm{i}\partial_t \psi = -\Delta\psi + \mathrm{i}\lambda\psi,$$
$$\frac{\mathrm{d}H(\psi)}{\mathrm{d}t} = 0.$$

The above argument indicates that we should introduce an imaginary Lagrange multiplier. Based on this argument, we introduce a Lagrange multiplier term $\mathrm{i}\lambda\psi$ with λ real. In order to deal with the second derivative in time, we also introduce a new variable $u(\boldsymbol{x},t) = \varepsilon\partial_t\phi(\boldsymbol{x},t)$ to reformulate (4.23)-(4.25) as follows:

$$\mathrm{i}\partial_t\psi = -\Delta\psi - \phi\psi - \mathrm{i}\lambda\psi, \qquad \boldsymbol{x}\in\Omega, \quad t>0, \tag{4.27}$$
$$\varepsilon\partial_t u = \Delta\phi - \phi + |\psi|^2 - \rho u, \quad \boldsymbol{x}\in\Omega, \quad t>0, \tag{4.28}$$
$$\varepsilon\partial_t\phi = u, \qquad \boldsymbol{x}\in\Omega, \quad t>0, \tag{4.29}$$
$$\frac{\mathrm{d}E(t)}{\mathrm{d}t} = -\frac{\rho}{\varepsilon}\|u\|^2, \tag{4.30}$$
$$\frac{\mathrm{d}}{\mathrm{d}t}H(\psi) = 0. \tag{4.31}$$

Then we can construct the R-GSAV/LM scheme for (4.27)-(4.31) similar to the scheme (3.4)-(3.11) as follows: Given $(\psi^{n-k},u^{n-k},\phi^{n-k},R^{n-k}),\dots,(\psi^n,u^n,\phi^n,R^n)$, we compute $(\psi^{n+1},u^{n+1},\phi^{n+1},R^{n+1})$ via the following steps:

Step 1. Find a solution $\widetilde{\psi}^{n+1},u^{n+1},\phi^{n+1},\widetilde{R}^{n+1}$ by using the GSAV approach

$$\mathrm{i}\frac{\alpha_k\bar{\psi}^{n+1}-A_k(\psi^n)}{\delta t} = -\Delta\bar{\psi}^{n+1} - B_k(\phi^n\psi^n) - B_k(\mathrm{i}\lambda^n\psi^n), \tag{4.32}$$
$$\varepsilon\frac{\alpha_k\bar{u}^{n+1}-A_k(u^n)}{\delta t} = \Delta\bar{\phi}^{n+1} - \bar{\phi}^{n+1} + B_k\left(|\psi|^2\right) - \rho\bar{u}^{n+1}, \tag{4.33}$$
$$\varepsilon\frac{\alpha_k\bar{\phi}^{n+1}-A_k(\phi^n)}{\delta t} = \bar{u}^{n+1}, \tag{4.34}$$
$$\frac{1}{\delta t}\left(\widetilde{R}^{n+1}-R^n\right) = -\frac{\rho}{\varepsilon}\frac{\widetilde{R}^{n+1}}{E(\bar{\psi}^{n+1},\bar{u}^{n+1},\bar{\phi}^{n+1})}\|\bar{u}^{n+1}\|^2, \tag{4.35}$$
$$\xi_k^{n+1} = \frac{\widetilde{R}^{n+1}}{E(\bar{\psi}^{n+1},\bar{u}^{n+1},\bar{\phi}^{n+1})}, \quad \eta_k^{n+1} = 1-\left(1-\xi_k^{n+1}\right)^{k+1}, \tag{4.36}$$
$$\widetilde{\psi}^{n+1} = \eta_k^{n+1}\bar{\psi}^{n+1}, \quad u^{n+1} = \eta_k^{n+1}\bar{u}^{n+1}, \quad \phi^{n+1} = \eta_k^{n+1}\bar{\phi}^{n+1}. \tag{4.37}$$

Step 2. Compute $\boldsymbol{\phi}^{n+1}$ and λ^{n+1} from

$$\frac{\alpha_k(\psi^{n+1}-\widetilde{\psi}^{n+1})}{\delta t} = -\lambda^{n+1}\psi^{n+1} + B_k(\lambda^n\psi^n), \tag{4.38}$$

$$H(\psi^{n+1}) = H(\psi^0). \tag{4.39}$$

Step 3. Update the SAV R^{n+1} via the following relaxation:

$$R^{n+1} = \zeta_0^{n+1}\widetilde{R}^{n+1} + \left(1-\zeta_0^{n+1}\right)E\left(\psi^{n+1}, u^{n+1}, \phi^{n+1}\right), \quad \zeta_0^{n+1} \in \mathscr{V}, \tag{4.40}$$

where

$$\mathscr{V} = \left\{\zeta \in [0,1] \ s.t. \ \frac{R^{n+1}-\widetilde{R}^{n+1}}{\delta t} = -\gamma^{n+1}\frac{\rho}{\varepsilon}\|u^{n+1}\|^2 + \frac{\rho}{\varepsilon}\frac{\widetilde{R}^{n+1}}{E(\bar{\psi}^{n+1}, \bar{u}^{n+1}, \bar{\phi}^{n+1})}\|\bar{u}^{n+1}\|^2\right\} \tag{4.41}$$

with $\gamma^{n+1} \geq 0$ to be determined so that $\mathscr{V}$ is not empty.

The above scheme can be implemented similarly as the scheme (3.4)-(3.11), and we can also establish stability results similar to those presented in Theorem 3.1. We leave the detail to the interested readers.

We now present some numerical results by using the above scheme. We first examine the temporal convergence rates.

Example 4.7. We include an external force in KGS equation (4.23)-(4.25) to make the exact solution be

$$\psi_\pm(x,t) = 3B\,\mathrm{sech}^2(Bx + c_\pm t)\exp\left[\mathrm{i}\left(d_\pm x + (4B^2 - d_\pm^2)t\right)\right], \tag{4.42}$$

$$\phi_\pm(x,t) = 6B^2\,\mathrm{sech}^2(Bx + c_\pm t), \quad x \in \mathbb{R}, \quad t \geq 0, \tag{4.43}$$

where $B \geq 0$ and

$$c_\pm = \pm\frac{\sqrt{4B^2-1}}{2\varepsilon} = \mathscr{O}\left(\frac{1}{\varepsilon}\right), \quad d_\pm = \mp\frac{\sqrt{4B^2-1}}{4B\varepsilon} = -\frac{c_\pm}{2B} = \mathscr{O}\left(\frac{1}{\varepsilon}\right).$$

The exact solution is chosen as

$$\psi(x,t) = \psi_+(x,t), \quad \phi(x) = \phi_+(x,t), \quad u(x,t) = \epsilon\partial_t\phi_+(x,t). \tag{4.44}$$

In our computation, we take $B = 1, \varepsilon = 1, \rho = 0.01$ and solve the problem on the interval $[-32, 32]$. We choose 1024 Fourier modes — i.e. spatial step $h = 1/16$, so that the spatial error is negligible compared with time discretization error. The errors based on discrete L^2-norm are shown in Fig. 10 which shows the expected accuracy.

Example 4.8. The initial data is chosen as

$$\psi^{(0)}(x) = \psi_+(x,0), \quad \phi^{(0)}(x) = \phi_+(x,0), \quad u^{(0)}(x) = \epsilon\partial_t\phi_+(x,0).$$

We simulate the propagation of a single solitary wave with $B = 1, \epsilon = 0.1, \rho = 0.1$ in the computational domain $[-40, 40]$. We set 1024 Fourier modes — i.e. spatial step $h = 5/64$, and $\delta t = 10^{-4}$. The results computed by R-GSAV/LM BDFk ($k = 1, 2, 3, 4$) schemes are shown in Fig. 11.

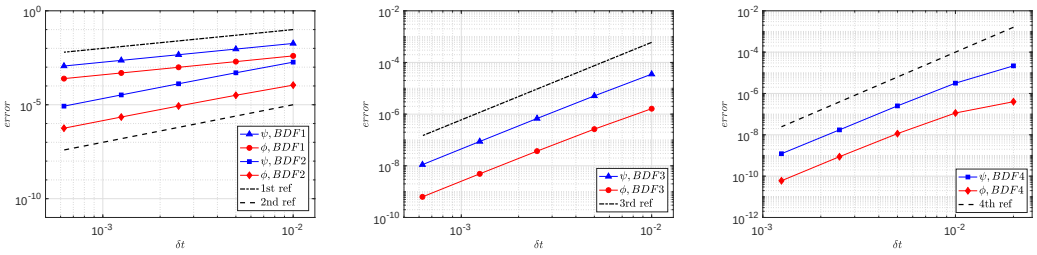

Figure 10: Example 4.7. Accuracy of solving KGS equations. Left: First- and second-order schemes. Middle: Third-order scheme. Right: Fourth-order scheme.

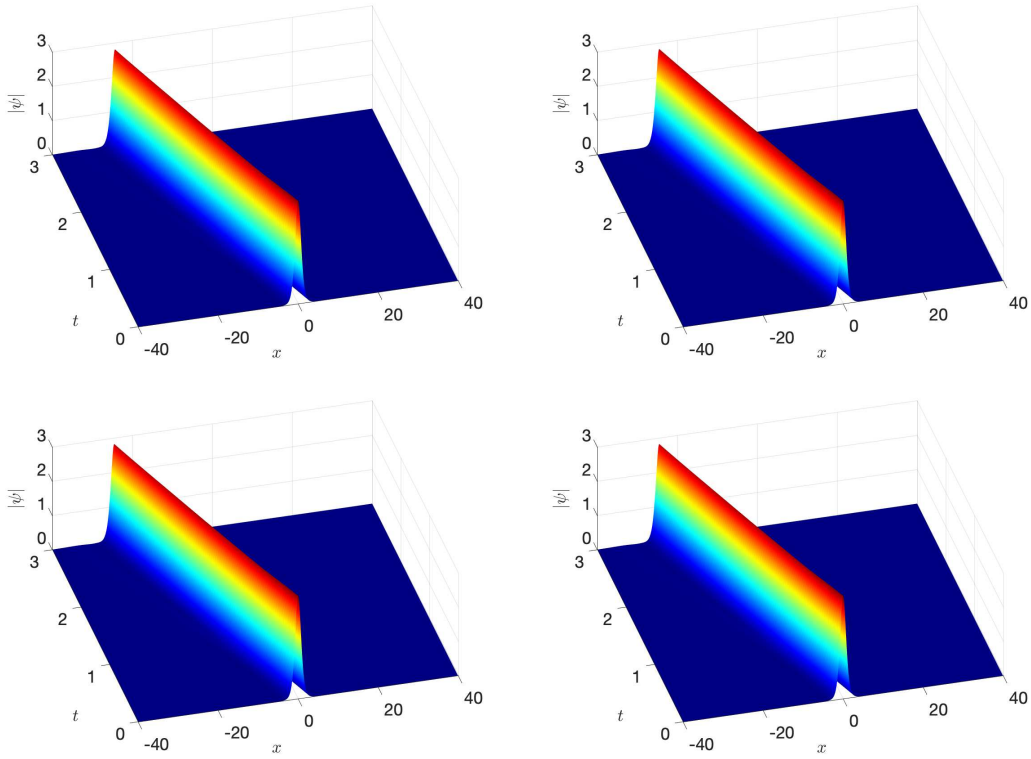

Figure 11: Example 4.8. Propagation of a single solitary wave computed by the R-GSAV/LM BDFk ($k=1,2,3,4$) schemes.

Example 4.9. We simulate the head-on collisions of solitary-wave solutions of KGS in 1D with $\varepsilon=1$ and $\rho=0.01,0.1,0.5$. The initial condition is chosen as

$$\begin{aligned}\psi(x,0)&=\psi_+(B,x-p,0)+\psi_-(B,x+p,0),\\ \phi(x,0)&=\phi_+(B,x-p,0)+\phi_-(B,x+p,0),\\ \partial_t\phi(x,0)&=\partial_t\phi_+(B,x-p,0)+\partial_t\phi_-(B,x+p,0),\end{aligned}$$

where $\psi_\pm$ and $\phi_\pm$ are defined as in (4.42)-(4.43), and $x=\pm p$ are initial locations of the

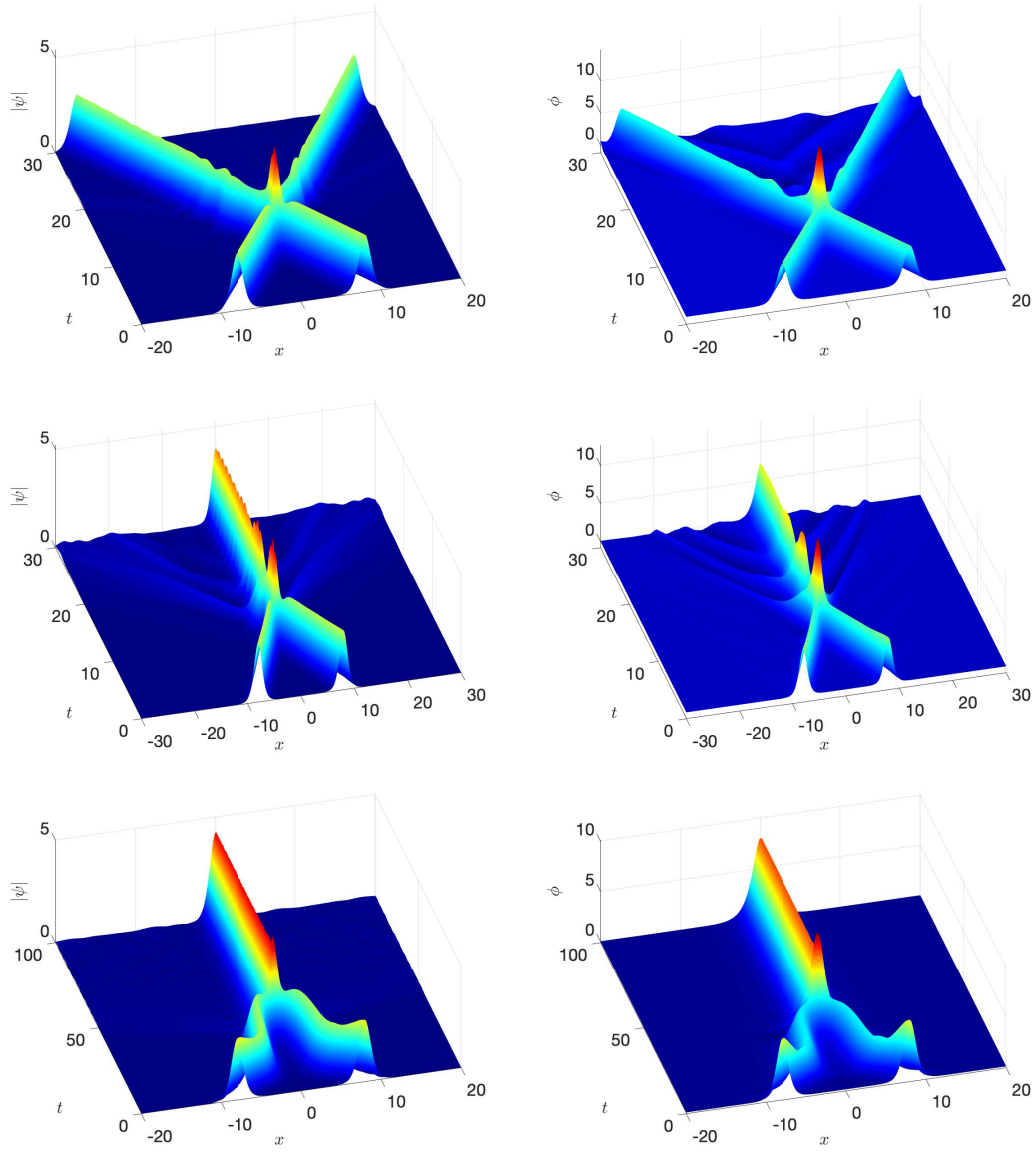

Figure 12: Example 4.9. Head-on collisions of two symmetric solitary waves. Left: Nucleon density ψ. Right: Meson field. From top to bottom: $\rho = 0.01$, $\rho = 0.1$, $\rho = 0.5$.

two solitons. We set $p = 8$, $B = 1$, and use the second-order R-GSAV/LM scheme to solve the problem in the interval $[-40, 40]$ with 2048 Fourier modes — i.e. mesh size $h = 5/128$, time step $\delta t = 10^{-3}$.

We plot in Fig. 12 the time evolution of $|\psi(x,t)|$ and $|\phi(x,t)|$ for different values of ρ, and plot in Fig. 13 the time evolution of the absolute value of Lagrange multiplier and energy for different values of ρ. These results are consistent with [28].

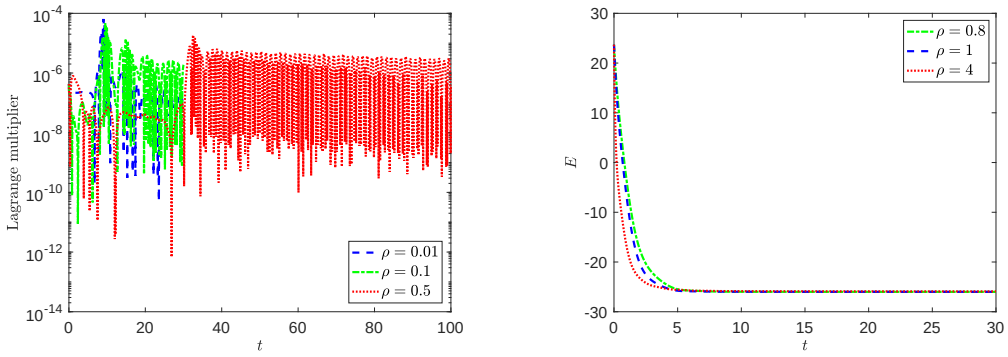

Figure 13: Example 4.9. Left: Evolutions of the absolute value of Lagrange multiplier. Right: Evolution of the energy.

Example 4.10. We simulate a dynamic process of KGS in 2D with $\rho = 1$ and $\varepsilon = 1$. The initial condition is taken as

$$\psi(x,y,0) = \frac{2}{e^{x^2+2y^2} + e^{-(x^2+2y^2)}} e^{i5/\cosh(\sqrt{4x^2+y^2})},$$
$$\phi(x,y,0) = e^{-(x^2+y^2)}, \quad \phi_t(x,y,0) = \frac{e^{-(x^2+y^2)}}{2}.$$

We use the second-order R-GSAV/LM scheme to solve this problem on the rectangle domain $[-64,64]^2$ with mesh size $h = 1/16$ and time step $\delta t = 10^{-3}$. Fig. 14 shows the surface plots of $|\psi|^2$ and ϕ at various times. We observe that these are similar to the conserved case with $\rho = 0$ reported in [4, 28]. We also plot the error of wave energy and ζ_0^{n+1} in Fig. 15. We observe that the wave energy is conserved exactly, and $\zeta_0^{n+1} \equiv 0$ which indicates that the scheme is energy dissipative with the original energy.

5. Conclusion

In this paper, we developed a new class of efficient schemes, termed as R-GSAV/LM schemes, for dissipative systems with global constraints. The schemes combine the main ideas of the relaxed generalized SAV approach [15, 17, 29] and the Lagrange multiplier approach [8], enjoy many distinct advantages compared with existing approaches, such as (i) more efficient as they only require solving one linear system with constant coefficients and one nonlinear algebraic system for the Lagrange multipliers only; (ii) can preserve global constraints exactly, and are unconditionally energy stable with a modified energy, which in most cases, equals to the original energy; and (iii) can be applied to a large class of dissipative systems with global constraints. We applied the R-GSAV/LM approach to a variety of problems to demonstrate its effectiveness and advantages compared with existing approaches.

While the new R-GSAV/LM approach enjoy many advantages, there are still some issues which need to be addressed, such as (i) how to construct similar numerical schemes

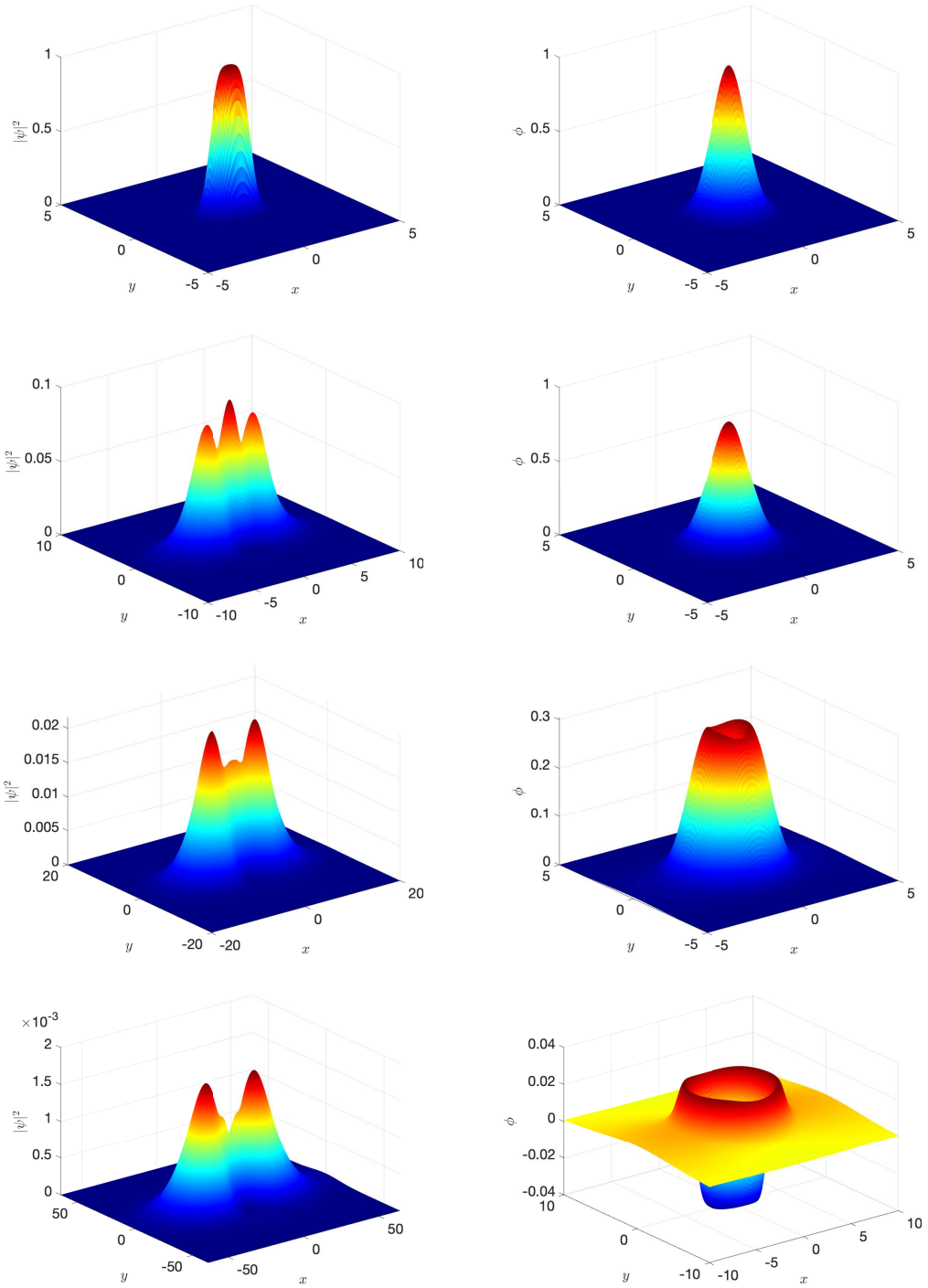

Figure 14: Example 4.10. Left: Surface of nucleon density $|\psi|^2$. Right: Meson field ϕ. From top to bottom: $T = 0$, $T = 0.5$, $T = 1$, $T = 3.5$.

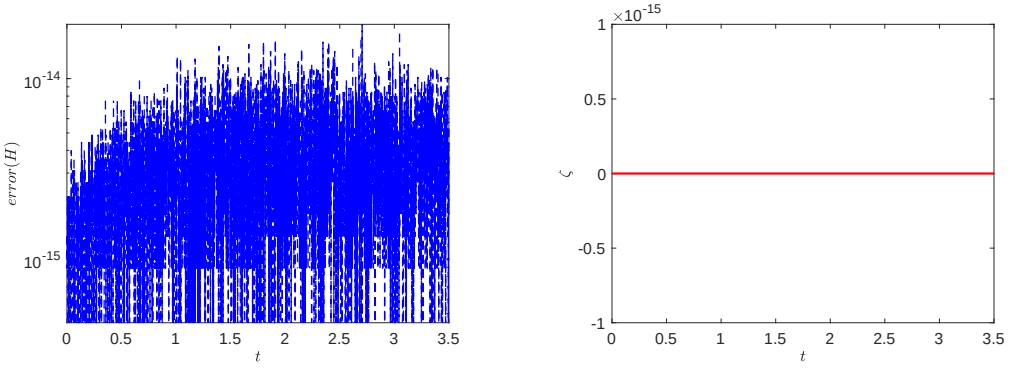

Figure 15: Example 4.10. KGS equations. Left: Error of the wave energy. Right: ζ_0^{n+1}.

for conservative systems with global constraints; (ii) how to deal with more complicated constraints; (iii) how to establish the well posedness for the nonlinear algebraic system involved in the scheme, and derive a rigorous error estimate. These subjects are worth studying in a future work.

Acknowledgments

This work is supported in part by NSFC 11971407.

References

[1] X. Antoine, J. Shen and Q. Tang, *Scalar Auxiliary Variable/Lagrange multiplier based pseudospectral schemes for the dynamics of nonlinear Schrödinger/Gross-Pitaevskii equations*, J. Comput. Phys. **437**, 110328 (2021).
[2] S. Ashhab and C. Lobo, *External Josephson effect in Bose-Einstein condensates with a spin degree of freedom*, Phys. Rev. A **66**, 013609 (2002).
[3] W. Bao and Q. Du, *Computing the ground state solution of Bose-Einstein condensates by a normalized gradient flow*, SIAM J. Sci. Comput. **25**, 1674–1697 (2004).
[4] W. Bao and L. Yang, *Efficient and accurate numerical methods for the Klein-Gordon-Schrödinger equations*, J. Comput. Phys. **225**, 1863–1893 (2007).
[5] L. Cafferelli and F. Lin, *An optimal partition problem for eigenvalues*, J. Sci. Comput. **31**, 5–18 (2007).
[6] L. Caffarelli and F. Lin, *Nonlocal heat flows preserving the L^2 energy*, Discrete Contin. Dyn. Syst. **23**, 49 (2009).
[7] Q. Cheng and J. Shen, *Multiple scalar auxiliary variable (MSAV) approach and its application to the phase-field vesicle membrane model*, SIAM J. Sci. Comput. **40**, A3982–A4006 (2018).
[8] Q. Cheng and J. Shen, *Global constraints preserving scalar auxiliary variable schemes for gradient flows*, SIAM J. Sci. Comput. **42**, A2489–A2513 (2020).
[9] Q. Cheng and J. Shen, *A new Lagrange multiplier approach for constructing structure preserving schemes, I. Positivity preserving*, Comput. Methods Appl. Mech. Engrg. **391**, 114585 (2022).
[10] Q. Cheng and J. Shen, *A new Lagrange multiplier approach for constructing structure preserving schemes, II. Bound preserving*, SIAM J. Numer. Anal. **60**, 970–998 (2022).

[11] Q. Du and X. Feng, *The phase field method for geometric moving interfaces and their numerical approximations*, in: *Geometric partial differential equations. Part I*, pp. 425–508, Elsevier/North-Holland (2020).
[12] Q. Du and F. Lin, *Numerical approximations of a norm-preserving gradient flow and applications to an optimal partition problem*, Nonlinearity **22**, 67 (2008).
[13] C.M. Elliott and A.M. Stuart, *The global dynamics of discrete semilinear parabolic equations*, SIAM J. Numer. Anal. **30**, 1622–1663 (1993).
[14] J.L. Guermond, P. Minev and J. Shen, *An overview of projection methods for incompressible flows*, Comput. Methods Appl. Mech. Engrg. **195**, 6011–6045 (2006).
[15] F. Huang and J. Shen, *A new class of implicit-explicit BDFk SAV schemes for general dissipative systems and their error analysis*, Comput. Methods Appl. Mech. Engrg. **392**, 114718 (2022).
[16] F. Huang, J. Shen and Z. Yang, *A highly efficient and accurate new scalar auxiliary variable approach for gradient flows*, SIAM J. Sci. Comput. **42**, A2514–A2536 (2020).
[17] M. Jiang, Z. Zhang and J. Zhao, *Improving the accuracy and consistency of the scalar auxiliary variable (SAV) method with relaxation*, J. Comput. Phys. **456**, 110954 (2022).
[18] X. Jing and Q. Wang, *Linear second order energy stable schemes for phase field crystal growth models with nonlocal constraints*, Comput. Math. Appl. **79**, 764–788 (2020).
[19] J. Shen, T. Tang and J. Yang, *On the maximum principle preserving schemes for the generalized Allen-Cahn equation*, Commun. Math. Sci. **14**, 1517–1534 (2016).
[20] J. Shen, C. Wang, X. Wang and S.M. Wise, *Second-order convex splitting schemes for gradient flows with Ehrlich-Schwoebel type energy: Application to thin film epitaxy*, SIAM J. Numer. Anal. **50**, 105–125 (2012).
[21] J. Shen, J. Xu and J. Yang, *The scalar auxiliary variable (SAV) approach for gradient flows*, J. Comput. Phys. **353**, 407–416 (2018).
[22] J. Shen, J. Xu and J. Yang, *A new class of efficient and robust energy stable schemes for gradient flows*, SIAM Rev. **61**, 474–506 (2019).
[23] J. Shen and X. Yang, *Numerical approximations of Allen-Cahn and Cahn-Hilliard equations*, Discrete Contin. Dyn. Syst. **28**, 1669 (2010).
[24] X. Wang, L. Ju and Q. Du, *Efficient and stable exponential time differencing Runge-Kutta methods for phase field elastic bending energy models*, J. Comput. Phys. **316**, 21–38 (2016).
[25] J. Williams, R. Walser, J. Cooper, E. Cornell and M. Holland, *Nonlinear Josephson-type oscillations of a driven, two-component Bose-Einstein condensate*, Phys. Rev. A **59**, R31 (1999).
[26] C. Xu and T. Tang, *Stability analysis of large time-stepping methods for epitaxial growth models*, SIAM J. Numer. Anal. **44**, 1759–1779 (2006).
[27] X. Yang and L. Ju, *Efficient linear schemes with unconditional energy stability for the phase field elastic bending energy model*, Comput. Methods Appl. Mech. Engrg. **315**, 691–712 (2017).
[28] Y. Zhang and J. Shen, *Efficient structure preserving schemes for the Klein-Gordon-Schrödinger equations*, J. Sci. Comput. **89**, 1–26 (2021).
[29] Y. Zhang and J. Shen, *A generalized SAV approach with relaxation for dissipative systems*, J. Comput. Phys. **464**, 111311 (2022).
[30] Q. Zhuang and J. Shen, *Efficient SAV approach for imaginary time gradient flows with applications to one-and multi-component Bose-Einstein Condensates*, J. Comput. Phys. **396**, 72–88 (2019).